J Biol Inorg Chem (2014) 19:1367–1376
DOI 10.1007/s00775-014-1195-5

ORIGINAL PAPER

NMR chemical shift study of the interaction of selected peptides with liposomal and micellar models of apoptotic cells

Aurore Van Koninckxloo · Céline Henoumont · Sophie Laurent · Robert N. Muller · Luce Vander Elst

Received: 1 July 2014 / Accepted: 12 September 2014 / Published online: 7 October 2014

Abstract The interaction between two peptides previously selected by phage display to target apoptotic cells and phospholipidic models of these cells (liposomes or micelles made of 1,2-dipalmitoyl-sn-glycero-3-phosphocholine (DPPC) and/or 1,2-dipalmitoyl-sn-glycero-3-phospho-L-serine (DPPS, phosphatidylserine analog) was studied by the simple analysis of the changes induced on the proton NMR chemical shifts of the peptides. Our approach which does not need healthy and/or apoptotic cells for assessing the affinity of different peptides is fast and efficient and requires small amounts of peptide to determine the association constant, the interacting protons, and the number of interaction sites. The micellar model gave more reliable results than the liposomal one. The preferential interaction of the peptide with DPPS was evidenced by the change of the chemical shifts of specific amino acids of the peptides. Our micellar model is thus well suited to mimic apoptotic cells.

Keywords NMR · Phospholipidic model · Interaction · Apoptose · Phosphatidylserine

Electronic supplementary material The online version of this article (doi:10.1007/s00775-014-1195-5) contains supplementary material, which is available to authorized users.

A. Van Koninckxloo · C. Henoumont · S. Laurent · R. N. Muller · L. Vander Elst (✉)
Department of General, Organic and Biomedical Chemistry, NMR and Molecular Imaging Laboratory, University of Mons, 7000 Mons, Belgium
e-mail: luce.vanderelst@umons.ac.be

R. N. Muller · L. Vander Elst
CMMI-Center for Microscopy and Molecular Imaging, Rue Adrienne Bolland, 8, 6041 Gosselies, Belgium

Introduction

Apoptosis, or programmed cell death, is essential for tissue development and maintenance of cellular homeostasis. Insufficient apoptosis plays a key role in the pathogenesis of various disorders such as cancer or autoimmune diseases [1], whereas a high level of apoptotic activity is associated with myocardial infarction [2], neurodegenerative diseases (such as Alzheimer, Parkinson and Huntington diseases [3]) and advanced atherosclerotic lesions [4].

One of the most prominent biochemical hallmarks of apoptosis is a modification of the plasma membrane, with the exposure of phosphatidylserine (PS) in the outer leaflet of the cell membrane. The exposure of PS is responsible for macrophages recognition [5] and absorption of surrounding apoptotic cells without induction of inflammatory response.

Annexin V is a well-known protein that binds to PS [6]. Annexin V may be conjugated to different molecules and serves as a sensitive probe which allows seeing the anchoring of the protein by fluorescence microscopy [7], flow cytometry [8] and MRI techniques [9].

There are limitations using Annexin V among which cost, size, calcium-dependent protein and binding to necrotic cells in vitro are examples. Since 2006, the substitution of large proteins by small peptides as vector of apoptotic cells to circumvent these disadvantages appeared [10, 11].

One of the goals of the research of our team is to identify specific peptide vectors for molecular imaging. In this perspective, the phage display technique was used to select two peptides able to target apoptosis, the linear hexapeptides E3 (TVLSSL) and R826 (LIKKPF) [12, 13]. Assessing the affinity of the peptide for its target is an essential part of the study of its specificity. Ideally, the affinity should be tested against apoptotic and healthy cells.

However, induction of apoptosis and the quantification of the percentage of apoptotic cells is quite laborious and a constant level of apoptosis is difficult to maintain during the experiment. Consequently, in most experiments, the specific target i.e., PS has been used. A wide range of techniques can be used to determine binding constants. In most of them, the target is immobilized on a surface (e.g., bio-layer interferometry [14], surface plasmon resonance [15, 16], ELISA), whereas other ones use peptide grafted with fluorescence agent (confocal microscopy [17]). To mimic more precisely the curvature of the cells and thus the natural environment and to avoid modification of the peptide by grafting a tail to one of its terminal part, we propose in this paper to design an artificial membrane model mimicking apoptotic cells without needing of cell culture and allowing to determine an association constant by a simple and easy way. We developed thus phospholipidic models and studied the interaction of both peptides already known to target apoptotic cells by a ^{1}H NMR common sequence. Phospholipids systems (liposomes, micelles) have been chosen since they are widely used for over 30 years to mimic biological membranes in various fields (e.g., study of membrane fusion [18], study of cell membrane properties [19]). Recently, Kapty et al. [17] published a similar approach for the study of peptide binding to PS using liposomes and microscopy to determine the dissociation constant.

In the present work, we simply analyzed the proton NMR chemical shift changes for the evaluation of the non-covalent interactions between the targeting vector and PS containing micelles/liposomes. This method is fast, reproducible and reliable and requires small amounts of peptide to predict the association constant. Two other additional useful information can be derived with this technique: which protons are interacting and how many sites of interaction are present.

We compare liposomes to micelles as a model of apoptotic cells to determine the most appropriate model. The peptides E3 and R826 and their scramble analogs (same amino acids but in a different order) were used to prove the specificity of the interaction.

In this study, peptide concentration is kept constant while the concentration of phospholipids is variable. The obtained titration curves allow extracting the association parameters.

Materials and methods

General

1,2-Dipalmitoyl-sn-glycero-phosphatidylcholine (DPPC) and 1,2-dipalmitoyl-sn-glycero-3-phospho-L-serine (DPPS) were purchased from Genzyme Pharmaceuticals (Liesta, Switzerland). Cholesterol and other compounds were obtained from Sigma Aldrich (Bornem, Belgium). Peptides were synthesized by PolyPeptide group (Strasbourg, France).

Preparation of liposomes and micelles

Liposomes and micelles are formed by DPPC and/or DPPS. Liposomes are prepared by a conventional thin film-hydration method, as described previously [20]. Briefly, DPPC, DPPS and cholesterol (64/16/20 w/w) or DPPC and cholesterol (80/20 w/w) were dissolved in 4:1 (v/v) chloroform/methanol solution. Mixture was evaporated at 323 K until organic solvent was completely removed. Deuterated water was added to dissolve the thin film at 323 K. Liposome size was adjusted to around 100 nm using extruding equipment. The lipid suspension was extruded ten times through two stacked filters (Nucleopore Track-Etch Membrane, 800, 400, 200 and 100 nm pore size, Whatman plc, UK).

Micelles are prepared in the same way except extrusion and composition [21]. Thin film of phospholipids (DPPS or DPPC) is rehydrated with deuterated water and the solution is sonicated during 15 min while maintaining the temperature at 328 K with a thermostatic bath. 8 mg of Tween® 80 is added and the suspension is sonicated to obtain micelles with a size ranging typically between 20 and 100 nm. Micelles mimicking apoptotic cells are composed of DPPS and Tween® 80. Healthy cells are mimicked by DPPC micelles and Tween® 80.

Determination of liposomes/micelles size and zeta potential

The average diameter and size distribution of liposomes and micelles were measured on a Zetasizer NanoS Photon Correlation Spectroscopy by dynamic light scattering method (Malvern instrument, United Kingdom) at room temperature. The zeta potential of micelles and liposomes was measured on the same instrument. Measurements were performed at 298 K and pH 7 using a standard capillary cell.

Liposome and micelle stability

Liposome stability was analyzed through the potential change of the diameter and polydispersity index (PDI) over time. The PDI represents the width of the particle size distribution. A PDI value close to zero is observed for a monodisperse distribution. After 15 days, vesicles composed of DPPC and DPPS (80/20 w/w) extruded 10 times have the same size and same PDI. The diameter of

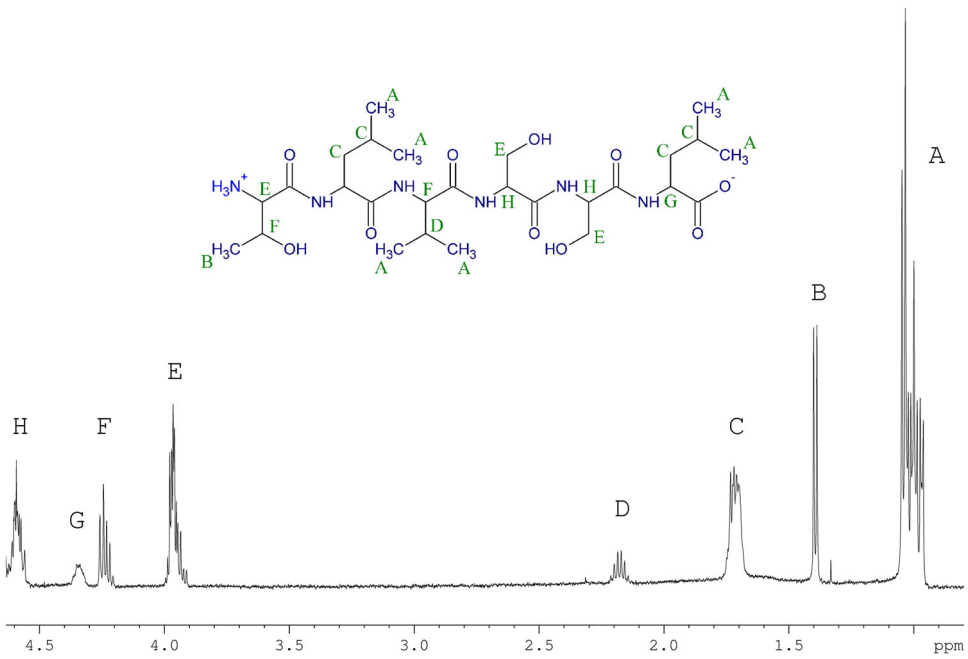

Fig. 1 ^{1}H NMR spectrum of E3 peptide: (D_2O, [E3 peptide] = 0.5 mM, δ ppm; m, multiplet; t, triplet; d, doublet): *A* 0.96–1.08 (m, 18H, 6 × CH_3); *B* 1.4 (d, $J = 6.7$ Hz 3H, 1 × CH_3); *C* 1.68–1.76 (m, 6H, 2 × CH_2, 2 × CH); *D* 2.15–2.23 (m, $J = 7$ Hz; 1H, 1 × CH); *E* 3.9–4.0 (m, 5H, 2 × CH_2, 1 × CH); *F* 4.2–4.28 (m, $J = 7.15$, 6.3 Hz; 2H, 2 × CH); *G* 4.33–4.38 (m, 1H, 1 × CH); *H* 4.56–4.65 (m, 3H, 3 × CH)

liposomes made solely of DPPC is rising from 100 to 130 nm. There is no change in size for DPPC or DPPS micelles after 6 months, only a slight increase in PDI was observed.

Determination of phospholipids concentration

The lipid concentration is determined using the Bartlett assay modified by Barenholz [22, 23]. This assay is based on spectrophotometric determination of phosphate included in each phospholipidic model. After phosphate release with perchloric acid, inorganic phosphate is complexed with ammonium molybdate which is reduced to a blue-colored complex by ascorbic acid. The concentration of this compound is calculated from its absorbance at 800 nm. (Perkin Elmer Lambda 35 UV/VIS spectrometer, Brussels, Belgium).

^{1}H NMR spectra

The measurements were performed on an Avance II-500 spectrometer (Bruker, Karlsruhe, Germany) operating at 500 MHz. The temperature was maintained at 310 K. All the solutions were prepared in D_2O. All spectra were recorded with 128 scans, a recycle delay of 4.17 s and a flip angle of 30°. The peptide spectra in the presence of liposomes or micelles containing different concentrations of DPPS and DPPC were recorded. The first spectrum ([DPPS] = 0 mm) corresponds to DPPC liposomes or micelles. Chemical shifts of the peaks showing shifts in the presence of liposomes or micelles were used to determine the association constant.

Assignment of NMR spectra

E3 peptide and its scramble (TLVSSL and SVSLLT)

The ^{1}H NMR spectrum of the E3 peptide (Fig. 1) is characterized by eight complex signals, and 11 for the E3 scramble peptide (Fig. 2), the assignment of which was facilitated by the analysis of the COSY spectrum (Correlation Spectroscopy) (Fig. S1 and S2). ^{1}H chemical shifts were expressed in ppm and referred to H_2O residual peak fixed at 4.72 ppm (2360 Hz).

R826 peptide and its scramble (LIKKPF and FKIPKL)

The ^{1}H NMR spectrum of R826 peptide is characterized by 25 complex signals and 19 for R826 scramble peptide (Figs. 3, 4). To facilitate the assignment of the different signals observed in the ^{1}H spectra, 2D correlation type experiments—Correlation Spectroscopy (COSY) (Fig. S3 and S4) and Total Correlation Spectroscopy [TOCSY, also called "Homonuclear Hartman Hahn spectroscopy" (HOHAHA)]—were used. Figures 3 and 4 show the structures and spectra of the peptide R826 and its scramble, respectively, and the capital letters correspond to the various signals of the ^{1}H NMR spectrum.

Determination of affinity constant [24–26]

The binding process between the peptide (P) and the phospholipidic ligand (*L*) can be described by the Eq. (1):

$$[L] + [P] \rightleftharpoons [PL] \quad (1)$$

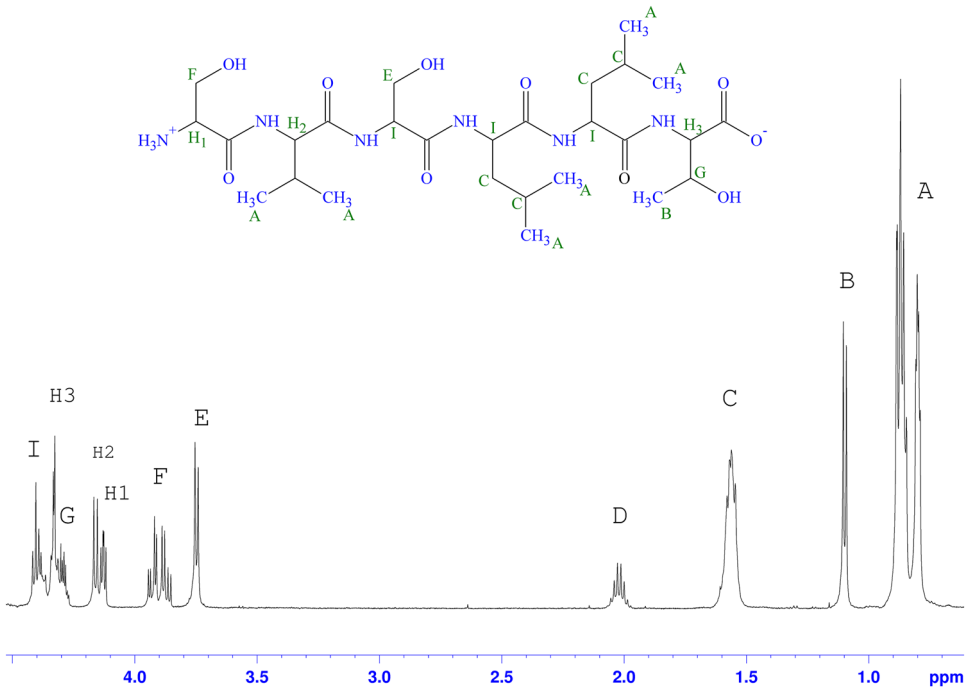

Fig. 2 ^{1}H NMR spectrum of E3 scramble peptide: (D_2O, [E3 scramble peptide] = 0.5 mM, δ ppm): *A* 0.81–0.95 (m, 18H, 6 × CH_3); *B* 1.11 (d, *J* = 6.15 Hz 3H, 1 × CH_3); *C* 1.52–1.64 (m, 6H, 2 × CH_2, 2 × CH); *D* 1.98–2.08 (m, *J* = 7 Hz; 1H, 1 × CH); *E* 3.76 (d, *J* = 6.6 Hz; 2H, 1 × CH_2); *F* 3.85–3.98 (dd, *J* = 4.8, 12.55 Hz; 2H, 1 × CH_2); *G* 4.28–4.32 (m, 1H, 1 × CH); H_1 4.14 (m, *J* = 5 Hz; 1H, 1 × CH); H_2 4.17 (d, *J* = 7.45 Hz; 1H, 1 × CH); H_3 4.34 (d, *J* = 3.5 Hz; 1H, 1 × CH); *I* 4.35–4.45 (m, 3H, 3 × CH)

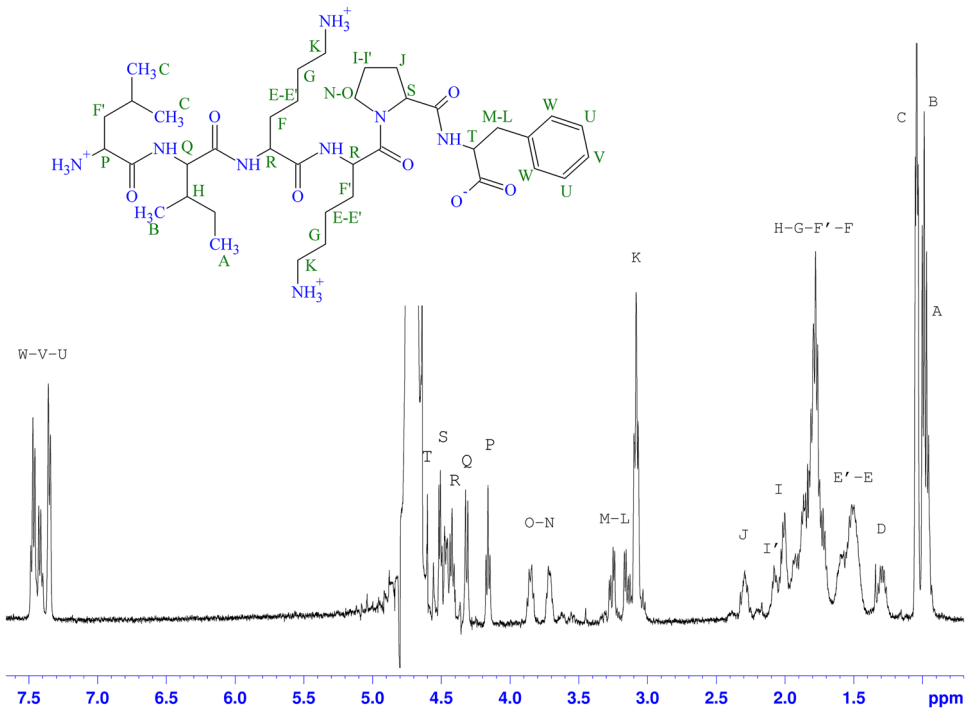

Fig. 3 ^{1}H NMR of R826 peptide: (D_2O; [R826 peptide] = 0.5 mM; δ ppm): *A* 0.96 (t, 3H, 1 × CH_3); *B* 0.995 (d, 3H, 1 × CH_3); *C* 1.05 (m, 6H, 2 × CH_3); *D* 1.24–1.36 (m, 2H, 1 × CH_2); *E*–*E*′ 1.42–1.65 (m, 4H, 2 × CH_2); *F*–*F*′–*G*–*H* 1.68–1.97 (m, 12H, 2 × CH, 5 × CH_2); *I*–*I*′ 1.97–2.13 (m, 2H, 1 × CH_2); *J* 2.24–2.34 (m, 2H, 1 × CH_2); *K* 3.08 (t, *J* = 7.1 Hz; 4H, 2 × CH_2); *L*–*M* 3.11–3.30 (dd, *J* = 5.9, 13.3 Hz; 2H, 1 × CH_2), *N*–*O* 3.67–3.89 (m, 2H, 1 × CH_2); *P* 4.16 (t, *J* = 7.1 Hz; 1H, 1 × CH); *Q* 4.32 (d, *J* = 8.35 Hz; 1H, 1 × CH); *R* 4.39–4.45 (m, 2H, 2 × CH), *S* 4.45–4.53 (m, 1H, 1 × CH), *T* 4.6 (t, *J* = 6 Hz; 1H, 1 × CH); *U*–*W* 7.32–7.5 (m, *J* = 7.45 Hz; 5H, 5 × CH)

The non-covalent interaction is an equilibrium reaction governed by the following equilibrium constant (Eq. 2):

$$K_a = \frac{[PL]}{[P] \times [L]} \quad (2)$$

where [*P*], [*L*], [*PL*] are the equilibrium concentrations of peptide, ligand and bound peptide, respectively.

P_0 and L_0 are the total concentrations of peptide and ligand, respectively.

$$P_0 = [PL] + [P] \quad (3)$$

$$L_0 = [PL] + [L] \quad (4)$$

By combining Eqs. (2), (3) and (4), Eq. (5) can be derived for one site of interaction.

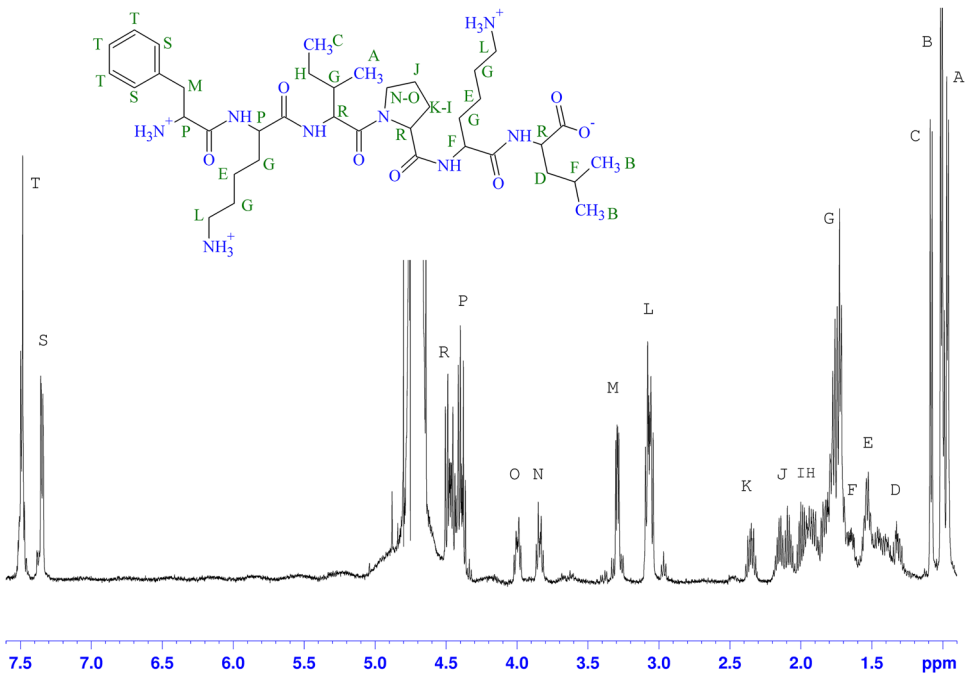

Fig. 4 ^{1}H NMR spectrum of R826 scramble peptide: (D_2O; [R826 scramble peptide] = 0.5 mM, δ ppm): *A–C* 0.96–1.08 (m, J = 6.6 Hz; 12H, 4 × CH_3); *D* 1.27–1.36 (m, 2H, 1 × CH_2); *E* 1.42–1.59 (m, 4H, 2 × CH_2); *F* 1.6–1.68 (m, 1H, 1 × CH); *G* 1.70–1.80 (m, 9H, 4 × CH_2, 1 × CH); *H* 1.8–1.95 (m, 2H, 1 × CH_2); *I* 1.96–2.04 and *K* 2.3–2.4 (m, 2H, 1 × CH_2); *J* 2.04–2.21 (m, 2H, 1 × CH_2); *L* 3.0–3.13 (dt, J = 7.5, 7.8 Hz; 4H, 2 × CH_2); *M* 3.24–3.34 (m, 2H, 1 × CH_2); *N–O* 3.8–4.05 (m, 2H, 1 × CH_2); *P* 4.35–4.44 (m, 3H, 3 × CH); *R* 4.44–4.54 (m, 3H, 3 × CH); *S* 7.35 (dd, J = 7.55, 2.0 Hz; 2H, 2 × CH); *T* 7.5 (m, J = 6.8 Hz; 3H, 3 × CH)

$$K_a = \frac{[PL]}{(P_0 - [PL]) \times (L_0 - [PL])} \quad (5)$$

If n independent and identical sites of interaction exist on the ligand, the total concentration of binding sites is nL_0 and the term $(L_0 - [PL])$ can be replaced by $(nL_0 - [PL])$.

The concentration of bound peptide $[PL]$ can then be calculated using the following equation:

$$[PL] = \frac{(K_a(P_0 + nL_0) + 1) \pm \sqrt{((K_a(P_0 + nL_0) + 1))^2 - 4 \times P_0 \times nL_0 \times K_a^2}}{2K_a} \quad (6)$$

The binding of peptide to PS was studied by the analysis of the changes of the ^{1}H NMR chemical shifts for L_0 ranging from 0.05 to 1.5 mM and P_0 fixed to 0.5 mM.

Chemical shifts are fitted by the following equations assuming a fast exchange between free and bound states of the peptide

$$\delta_0 = x_c \times \delta_c + (1 - x_c) \times \delta_f \quad (7)$$

$$\delta_0 = \left(\delta_f + \left(\frac{[PL]}{P_0}\right) \times (\delta_c - \delta_f)\right) \quad (8)$$

δ_o is the observed chemical shift at equilibrium, δ_c and δ_f are the chemical shifts of a nucleus in the bound peptide and in free peptide, respectively, and x_c is the molar fraction of bound peptides.

Results

Study of the interaction between liposomes and E3 or E3 scramble peptides

The hydrodynamic diameter of the DPPC–DPPS liposomes was close to 150 nm (Fig. S5) and the negative zeta potential (−65 mV) confirms the incorporation of PS in the outer layer of liposomes. The interaction was studied using a constant concentration of E3 peptide and a variable concentration of PS in the liposomal model. The actual concentration of PS outside liposomes was calculated assuming an equal proportion of PS in the inner and outer layers. Since the liposomes are composed of 20 % (w/w) of DPPS and 80 % of DPPC, it is thus estimated that only

$$\delta_0 = \delta_f + \left[\left(\frac{(K_a(P_0 + nL_0) + 1) \pm \sqrt{((K_a(P_0 + nL_0) + 1))^2 - 4 \times P_0 \times nL_0 \times K_a^2}}{2K_a P_o}\right) \times (\delta_c - \delta_f)\right] \quad (9)$$

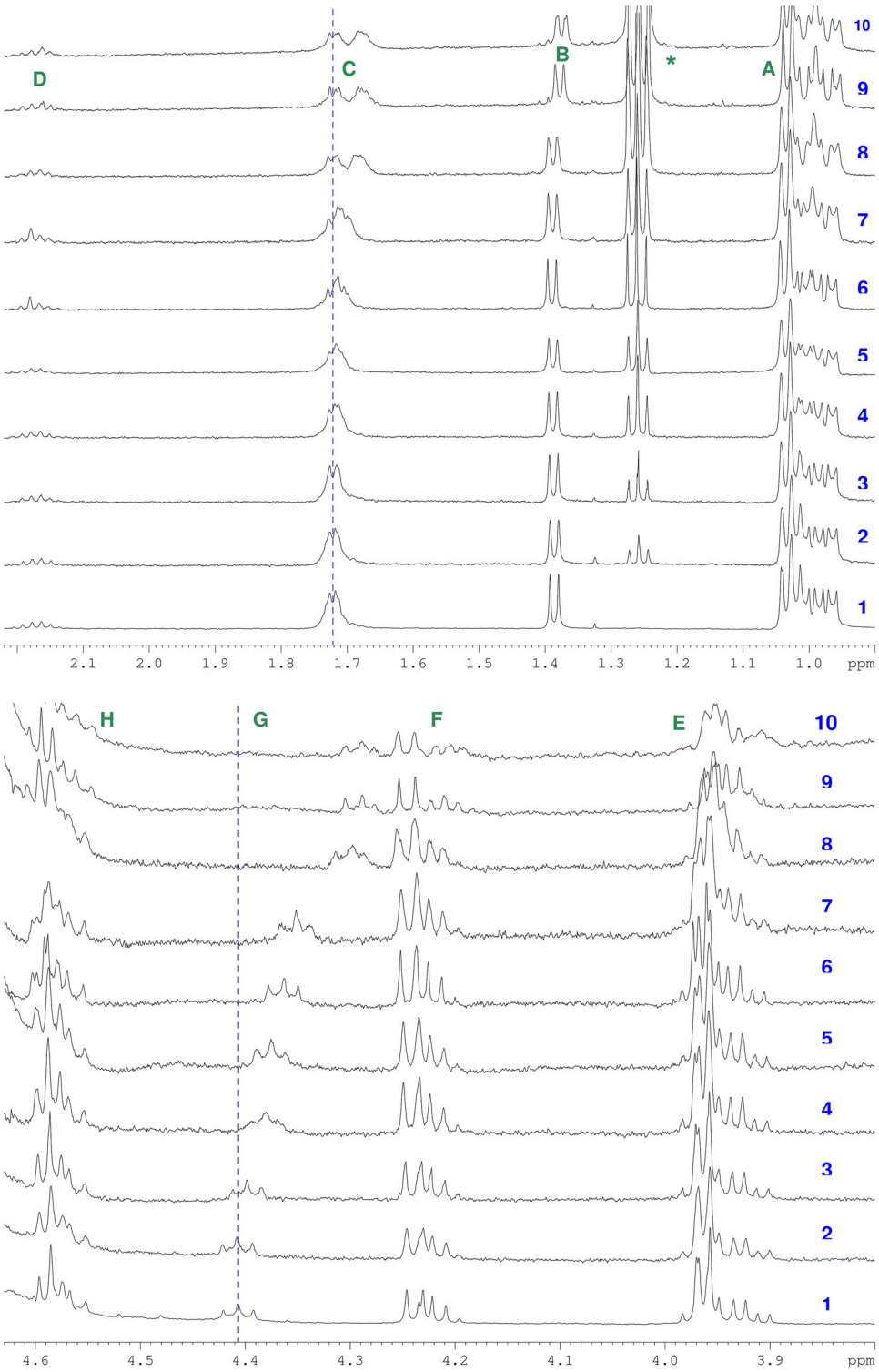

Fig. 5 Proton chemical shifts at pH 6.5 of E3 peptide 0.5 mM at 500 MHz (liposomal model). *1* E3 alone, *2* E3 + PC 0.75 mM, *3* E3 + PS 0.05 mM, *4* E3 + PS 0.125 mM, *5* E3 + PS 0.15 mM, *6* E3 + PS 0.175 mM, *7* E3 + PS = 0.2 mM, *8* E3 + PS = 0.5 mM, *9* E3 + PS 1.0 mM, *10* E3 + PS 1.5 mM, *resonances of the phospholipids

10 % of PS was in the outer layer of liposomes and thus able to interact with the peptide. This type of titration was preferred to avoid the possible influence of the peptide concentration on its chemical shifts. The PS concentration was varied by changing the liposomes concentration in the sample (Fig. 5). The point corresponding to zero concentration of PS is a sample containing E3 peptide and liposomes solely made of DPPC and mimicking healthy cells. These liposomes have similar size as the previous ones (100 nm) (Fig. S6) and their zeta potential is equal to zero.

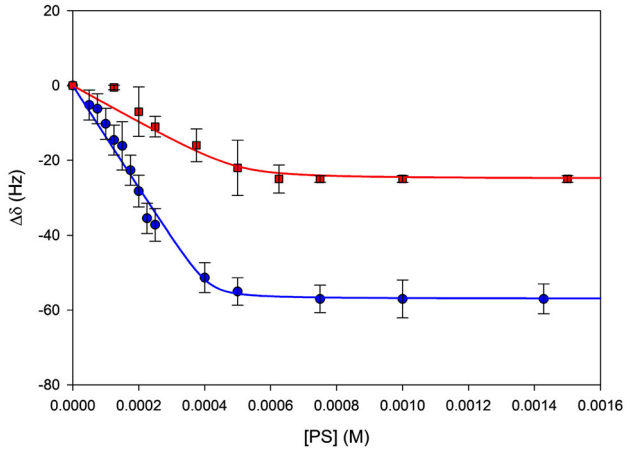

Fig. 6 Evolution of the chemical shift of G peak of E3 peptide (*dots*) and of the chemical shift of F peak of E3 scramble peptide (*squares*) as a function of PS concentration in the liposomal model. The *lines* correspond to the theoretical fittings using Eq. (9) (mean values ± SD)

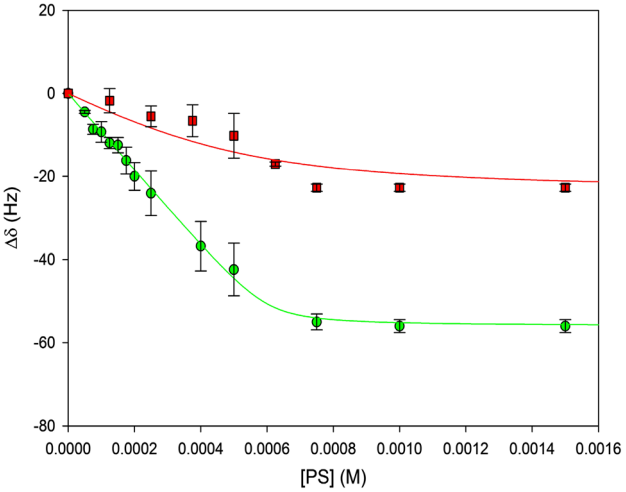

Fig. 7 Evolution of the chemical shift of G peak of the C-terminal leucine of E3 peptide (*dots*) and of the chemical shift of F peak of N-terminal serine of E3 scramble peptide (*squares*) as a function of PS concentration in the micellar model. The *lines* correspond to the theoretical fittings using Eq. (9) (mean values ± SD)

No chemical shift change was observed when pure DPPC liposomes were used, whereas the presence of PS induces shifts of several peaks.

By fixing the peptide concentration while increasing the amount of PS, some peaks clearly present either change of their shape and/or of their chemical shifts. This is the case for B, C, E, F and G peaks.

The experimental data obtained for G peak (C-terminal leucine) which shows the largest change in chemical shifts (δ around 4.35 ppm) were fitted using Eq. (9) to obtain an estimation of the association constant and the number of binding sites.

The agreement between the fitted points and the experimental data is good and the association constant is equal to 2.98×10^5 M^{-1} for 1.2 interaction sites (Fig. 6).

To confirm the specificity of E3 peptide sequence for PS, E3 scramble peptide was tested as a negative control. E3 scramble peptide (SVSLLT) shows weak interaction by its C- and N-termini parts (F, G, H_1 and H_3 peaks). The association constant calculated from the chemical shift changes of protons F of the N-terminal serine which shows the largest change in chemical shift (Fig. 6) is 32 times lower than the K_a of the hexapeptide E3 in the presence of PS containing liposomes (9.30×10^3 M^{-1}, $n = 1$).

Study of the interaction between liposomes and R826 peptide

The same protocol was used to study the interaction of R826 peptide with PS. Chemical shifts or line widths changes were observed for P, K, M–L and C peaks. It seems thus that there is also an interaction between the C and N-terminal parts and ε protons of lysine residues of R826 peptide and PS. However, quantitative data could not be obtained because of the overlapping of the liposomal signals and the chemical shifts of the M–L peaks and of the quite small shifts of P, C and K peaks. One-dimensional NMR proton spectra and the liposomal model mimicking apoptotic cells allowed thus to show that the peptide interacts with PS but the association constant could not be determined.

Another phospholipidic model of apoptotic cells was thus developed and this model uses DPPC and DPPS micelles mixed together in different proportions. Healthy cells are mimicked by DPPC micelles, while the presence of DPPS micelles mimics the apoptosis.

Study of the interaction between micelles and E3 or E3 scramble peptides

The hydrodynamic diameter of the DPPC and DPPS micelles is ranging between 20 and 80 nm (Fig. S7 and S8) and a single population is observed. Zeta potentials of DPPC and DPPS micelles were equal to 0 and −50 mV, respectively. Chemical shift changes of E3 peptide protons were similar to those observed previously in the presence of liposomes with G peak of C-terminal leucine showing the largest shift changes. This confirms the interaction between the C-terminal part of the E3 peptide and PS. The association constant was calculated after analysis of the shifts of G peak (Fig. 7). The same experimental conditions were used: temperature, NMR equipment, peptide concentration for each sample (0.5 mM) and variation of the PS concentration. To study micelles as an apoptotic model, the total phospholipids concentration was kept

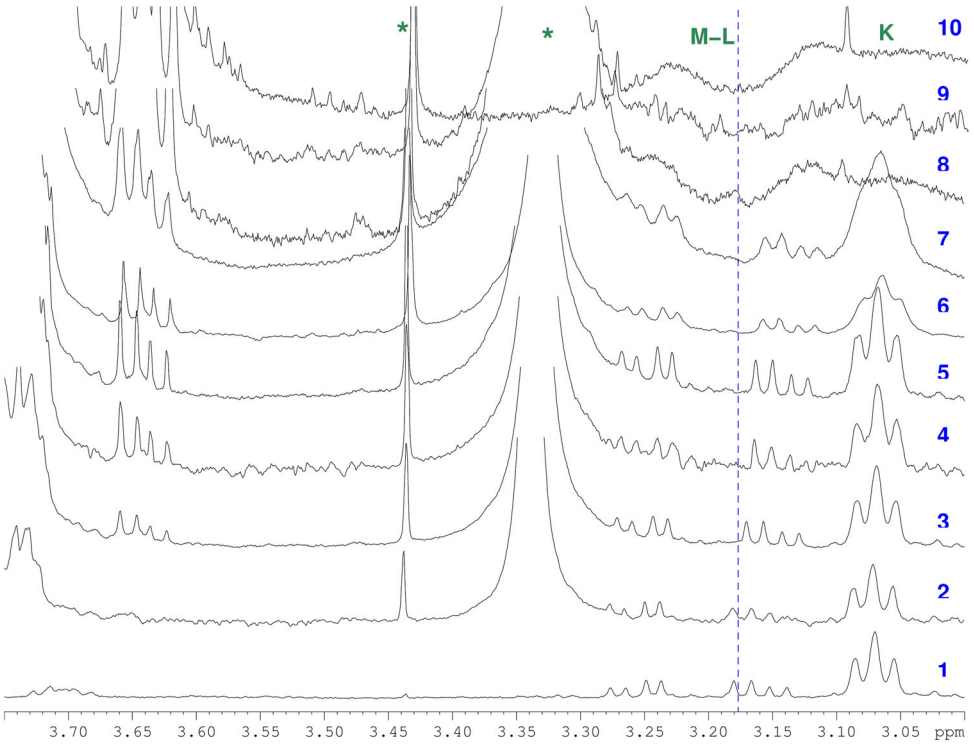

Fig. 8 Proton spectra of R826 peptide 0.5 mM pH 6.5 at 500 MHz. *1* R826 alone, *2* R826 + PC 1.5 mM, *3* R826 + PS 0.125 mM, *4* R826 + PS 0.2 mM, *5* R826 + PS 0.25 mM, *6* R826 + PS 0.3 mM, *7* R826 + PS 0.4 mM, *8* R826 + PS 0.75 mM, *9* R826 + PS 1 mM, *10* R826 + PS 1.5 mM, * resonances of the phospholipids

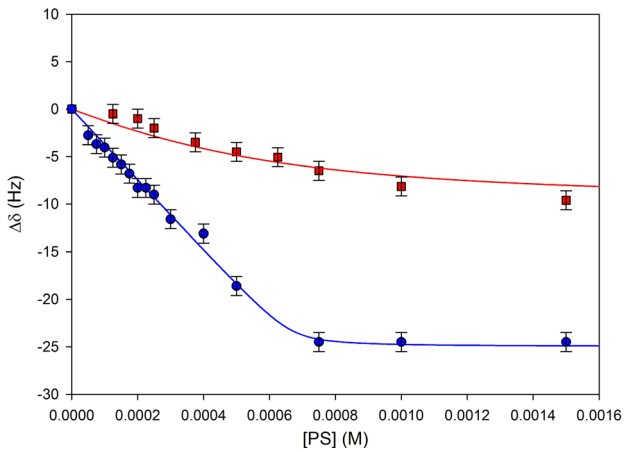

Fig. 9 Evolution of the chemical shifts of M–L peak (C-terminal phenylalanine) of R826 (*dots*) and of the N-terminal phenylalanine of R826 scramble (*squares*) as a function of PS concentration in the micellar model. The *lines* correspond to the theoretical fittings using Eq. (9) (mean values ± SD)

constant (1.5 mM) and only the ratio [PS]/[PC] was changed.

After fitting of the data, a K_a of 1.92×10^5 M^{-1} with $n = 0.83$ was obtained (Fig. 7).

Similarly to the experiments performed with liposomes, the K_a determined for the interaction between the E3 scramble peptide and PS in micelles is 6.93×10^3 M^{-1} for one site of interaction using the chemical shifts of the F peak.

Table 1 K_a values obtained for the four different peptides and the liposomal or micellar models

	K_a determined with liposomal model	K_a determined with micellar model
E3	$(2.98 \pm 4.2)\ 10^5\ M^{-1}$ ($n = 1.2 \pm 0.06$) ($R^2 = 0.985$)	$(1.92 \pm 1.1)\ 10^5\ M^{-1}$ ($n = 0.83 \pm 0.02$) ($R^2 = 0.997$)
E3 scramble	$(9.3 \pm 14.5)\ 10^3\ M^{-1}$ ($n = 1 \pm 0.15$) ($R^2 = 0.953$)	$(6.93 \pm 13.1)\ 10^3\ M^{-1}$ ($n = 1 \pm 0.8$) ($R^2 = 0.858$)
R826	–	$(3.89 \pm 4.0)\ 10^5\ M^{-1}$ ($n = 0.75 \pm 0.02$) ($R^2 = 0.994$)
R826 scramble	–	$(3.7 \pm 5.2)\ 10^3\ M^{-1}$ ($n = 1 \pm 0.8$) ($R^2 = 0.985$)

Study of the interaction between micelles and R826 or R826 scramble peptides

In these experiments, the shape and the chemical shifts of UVW, P, M–L, K, F and C peaks of R826 showed modifications (Fig. 8). These changes correspond to the protons of the C-and N-terminal parts as well as to the ε protons of lysine residues of the peptide, as found with liposomes. The most pronounced chemical shift is observed for the M–L peak corresponding to the C-terminal residue of the peptide. The association constant calculated from this shift

is equal to 3.89×10^5 M^{-1} (Fig. 9) with 0.75 site of interaction.

As observed in the study of peptide E3, the R826 scramble peptide has a lower interaction towards micelles. The shape and the chemical shifts of S–T, R, P and C peaks showed modifications. The affinity constant was calculated using the shifts of the S–T peaks of the aromatic N-terminal residue which shows the largest changes and is equal to 3.7×10^3 M^{-1} (Fig. 9) for one site of interaction.

Discussion

E3 and R826 which are known to bind to PS were used to test our models mimicking apoptotic cells: liposomal and micellar models. Both peptides and their scrambles were tested. Association constants (Table 1) were derived from the chemical shifts fitted according to the Eq. (9).

K_a for R826 peptide could not be determined with the liposomal model due to overlapping of the peaks corresponding to the liposome phospholipids and the C-terminal part of the peptide. Two-dimensional NMR spectra could have helped to discriminate the different peaks but our aim was to use simple 1D-NMR technique. A micellar model was thus developed and could be successfully used for all peptides.

Regarding the interaction between E3 peptide and the liposomal model, the association constant was found to be equal to 2.98×10^5 M^{-1} for 1.2 interaction sites. This value agrees with the apparent association constant of the E3 peptide previously determined by Elisa competition experiment with Annexin V ($K_a^* = 2.5 \times 10^6$ M^{-1}). The interaction of the analog E3 scramble peptide was 32 times lower than for E3 peptide showing the specificity of the E3 peptide.

With the micellar model, K_a of E3 scramble peptide was found to be 28 times lower than K_a of the E3 peptide. This ratio agrees quite well with the ratio obtained with the liposomal model. So, this micellar model of apoptotic cells confirms the specificity of E3 peptide as compared to its scramble analog.

The association constant between R826 and our micellar model is equal to 3.89×10^5 M^{-1}, whereas the scramble analog has a K_a 105 times lower. Recently, Kapty [17] reported a K_d of 0.69 μM ($K_a = 1.45 \times 10^6$ M^{-1}) for the PS interaction with R826 (LIKKPF) grafted with a fluorescein derivative on the N-terminus by fluorescence plate assay measurements. Burtea et al. [13] found an apparent dissociation constant K_d of 14.8 nM ($K_a = 6.76 \times 10^7$ M^{-1}) using competition ELISA experiments with Annexin V. The K_a obtained in our work is smaller than those reported values but is clearly related to a specific interaction of the peptide with PS.

The variation of the chemical shift changes of the peptides in the presence of liposomal and micellar models confirms that the E3 and R826 peptides interaction with phosphatidylserine is not purely electrostatic since the scramble peptides interaction with the target is much weaker. In case of pure electrostatic interaction, E3 peptide might interact by formation of a salt bridge between the carboxylic acid of leucine residue of the E3 peptide or threonine residue of the E3 scramble peptide and the amine moiety of phosphatidylserine. Conversely, the amine group of the N-terminal part of peptides could interact with carboxylic group of the serine ending group of DPPS phospholipids. The enhanced affinity of E3 compared to the scramble suggests that the conformation of the peptide plays an important role and more extensive calculation on the three-dimensional structure may help to confirm this hypothesis. The largest shifts observed for the C-terminal part of E3 result probably from its preferential interaction with DPPS.

Moreover, although the C-terminal amino acid of R826 scramble is identical to that of E3, the resonances of this amino acid shift to a lower extent than for E3, confirming that the interaction of these peptides with PS is not purely electrostatic.

For R826, the C-terminal amino acid (phenylalanine) seems to play a major role in the interaction. It is also to be noted that the increase of line width is larger for R826 than for E3 when interaction takes place. This suggests a more restricted motion of R826 when it is bound to the micelles.

It is also to be noticed that similar K_a values can be obtained on the other shifted peaks strengthening the reliability of the results.

Conclusions

E3 and R826 peptides were previously selected by phage display and their affinity for PS was determined by ELISA. This method involves several steps including immobilization of the target, incubation with an antibody coupled to peroxidase, rinsing and removal of unbound antibody, incubation with peroxidase substrate and measurement of the optical density. In the present study, the interaction of E3 and R826 peptides was tested on two phospholipidic models of apoptotic cells to determine their association constant using a simple NMR technique based on the analysis of the proton chemical shift changes. With the liposomal phospholipidic model of apoptotic cells, a K_a of 2.98×10^5 M^{-1} with 1.2 interaction sites was obtained for E3 peptide. The K_a is lower than that obtained by ELISA method but the experimental conditions are different. However, the

interaction seems definitely specific since E3 scramble peptide has a lower K_a value in the same conditions. No quantitative data could be obtained for the R826 peptide using this model because of an overlapping of different signals in the NMR spectra.

The micellar model gave K_a values closer to those values previously reported [13, 17] and allowed the study of the interaction of the R826 peptide which was not possible with the liposomal model. The association constants (K_a) obtained for the four peptides in the presence of the micellar apoptotic model showed that the interaction of E3 or R826 is higher than for their homologous scramble peptides. Moreover, this model needs less phospholipids than the liposomal one since in micellar structures, all phospholipids are exposed; whereas in liposome, only part of the phospholipids (about 50 %) is in contact with the external solution. The micellar model is thus an easy and low cost way to mimic apoptotic cells and to test their interaction with specific vectors.

Acknowledgments This work was supported by the Walloon Region (program First spin-off), the FNRS (*Fonds National de la Recherche Scientifique*), the UIAP VII and ARC Programs (AUWB-2010—10/15-UMONS-5) of the French Community of Belgium. The authors thank the Center for Microscopy and Molecular Imaging (CMMI, supported by the European Regional Development Fund and the Walloon Region).

Conflict of interest The authors declare no competing financial interest.

References

1. MacFarlane M, Williams AC (2004) EMBO Rep 5(7):674–678. doi:10.1038/sj.embor.7400191
2. Laufer EM, Reutelingsperger CPM, Narula J, Hofstra L (2008) Basic Res Cardiol 103:95–104. doi:10.1007/s00395-008-0701-8
3. Friedlander RM (2003) N Engl J Med 348(14):1365–1375
4. Mallat Z, Tedgui A (2001) Circ Res 88:998–1003. doi:10.1161/hh1001.090571
5. Fadok VA, De Cathelineau A, Daleke DL, Henson PM, Bratton DL (2001) J Biol Chem 276:1071–1077. doi:10.1074/jbc.M003649200
6. Van Tilborg GAF, Mulder WJM, Deckers N, Storm G, Reutelingsperger CPM, Strijkers GJ, Nicolay K (2006) Bioconjugate Chem 17:741–749. doi:10.1021/bc0600259
7. Baskic D, Popovic S, Ristic P, Arsenijevic NN (2006) Cell Biol Int 30:924–932. doi:10.1016/j.cellbi.2006.06.016
8. Koulov AV, Hanshaw RG, Stucker KA, Lakshmi C, Smith BD (2005) Isr J Chem 45:373–379. doi:10.1560/6AD4-LC9G-P57M-BE5Y
9. Van Tilborg GAF, Vucic E, Strijkers GJ, Cormode DP, Mani V, Skajaa T, Reutelingsperger CP, Fayad ZA, Mulder WJ, Nicolay K (2010) Bioconjug Chem 21(10):1794–1803. doi:10.1021/bc100091q
10. Hong H-Y, Choi JS, Kim YJ, Lee HY, Kwak W, Yoo J, Lee JT, Kwon T-H, Kim I-S, Han H-S, Lee B-H (2008) J Control Release 131:167–172. doi:10.1016/j.jconrel.2008.07.020
11. Thapa N, Kim S, So I-S, Lee B-H, Kwon I-C, Choi K, Kim I-S (2008) J Cell Mol Med 12(5A):1649–1660. doi:10.1111/j.1582-4934.2008.00305.x
12. Laumonier C, Segers J, Laurent S, Alain M, Coppée F, Belayew A, Vander Elst L, Muller RN (2006) J Biomol Screen 11(5):537–545. doi:10.1177/1087057106288220
13. Burtea C, Laurent S, Lancelot E, Ballet E, Murariu O, Rousseaux O, Port M, VanderElst L, Corot C, Muller RN (2009) Mol Pharm 6(6):1903–1919. doi:10.1021/mp900106m
14. Wallner J, Lhota G, Jeschek D, Mader A, Vorauer-Uhl K (2013) J Pharm Biomed Anal 72:150–154. doi:10.1016/j.jpba.2012.10.008
15. Abdiche YN, Myszka DG (2004) Anal Biochem 328:233–243. doi:10.1016/j.ab.2004.01.018
16. Baird CL, Courtenay ES, Myszka DG (2002) Anal Biochem 310:93–99. doi:10.1016/S0003-2697(02)00278-6
17. Kapty J, Banman S, Goping IS, Mercer JR (2012) J Biomol Screen 17(10):1293–1301. doi:10.1177/1087057112453313
18. Cypionka A, Stein A, Hernandez JM, Hippchen H, Jahn R, Walla PJ (2009) Proc Natl Acad Sci USA 106(44):18575–18580. doi:10.1073/pnas.0906677106
19. Campillo CC, Schroder AP, Marques CM, Pépin-Donat B (2009) Mater Sci Eng C 29:393–397. doi:10.1016/j.msec.2008.08.001
20. Lasic DD (1993) Liposomes: from physics to applications. Elsevier, Amsterdam
21. Parac-Vogt TN, Kimpe K, Laurent S, Piérart C, VanderElst L, Muller RN, Binnemans K (2006) Eur Biophys J 35:136–144. doi:10.1002/ejic.200400187
22. Bartlett GR (1959) J Biol Chem 234:466–468
23. Barenholz Y, Amselem S (1993) Quality control assays in the development and clinical use of liposome-based formulation. In: Gregoriadis G (ed) Liposome technology: liposome preparation and related techniques, 2nd edn. CRC, Boca Raton, pp 527–616
24. Fielding L, Rutherford S, Fletcher D (2005) Magn Reson Chem 43:463–470. doi:10.1002/mrc.1574
25. Fielding L (2007) Prog Nucl Magn Reson Spectrosc 51:219–242. doi:10.2174/1568026033392705
26. Luo R-S, Liu M-L, Mao X-A (1999) Spectrosc Acta Part A 55:1897–1901